

The Three-Body Potential for Heavy Quark Baryons in Lattice QCD

H. B. Thacker ¹

E. Eichten

Fermi National Accelerator Laboratory ²

P.O. Box 500, Batavia, Illinois 60610

J. C. Sexton ³

The Institute for Advanced Study

Princeton, New Jersey 08540

Abstract

The three-body static QQQ potential which binds a baryon composed of three heavy quarks is measured in lattice QCD. The data is well described by a sum of two-body $Q\bar{Q}$ meson potentials with no evidence for a three-body term. A conjugate gradient algorithm for calculating eigenvalues and eigenfunctions of the three-body Schrödinger equation is described.

¹ Talk delivered at the International Symposium on Field Theory of the Lattice, Seillac, France, Sept. 28-Oct. 3, 1987

² Fermilab is operated by Universities Research Association, Inc. under contract with the U.S. Department of Energy

³ Supported in part by DOE grant number DOE-AC02-76ER02220

The Three-Body Potential for Heavy Quark Baryons in Lattice QCD

H. B. Thacker

E. Eichten

Fermi National Accelerator Laboratory ¹

P.O. Box 500, Batavia, Illinois 60610

J. C. Sexton ²

The Institute for Advanced Study

Princeton, New Jersey 08540

Abstract

The three-body static QQQ potential which binds a baryon composed of three heavy quarks is measured in lattice QCD. The data is well described by a sum of two-body $Q\bar{Q}$ meson potentials with no evidence for a three-body term. A conjugate gradient algorithm for calculating eigenvalues and eigenfunctions of the three-body Schrödinger equation is described.

One of the simplest physical quantities in QCD which may be directly investigated by numerical lattice gauge techniques is the static potential between heavy quarks. For reasons of both simplicity and phenomenological relevance, the most extensively investigated case is that of the $Q\bar{Q}$ potential[1,2] $V(r)$ which determines the spectrum of a heavy quarkonium system. On the lattice, $V(r)$ may be obtained from the falloff of Wilson loops of width r and length t with t becoming large. In principle, it is straightforward to generalize this procedure to calculate the potential for any static color-singlet configuration of heavy quarks. For example, one may study the three-body QQQ potential[3] which binds a heavy quark baryon by studying the exponential falloff of a three-body Wilson loop depicted in Fig. 1. In this case, the exponent is proportional to the static three-quark potential $\mathcal{V}(\vec{r}_1, \vec{r}_2, \vec{r}_3)$.

There are several reasons why the QQQ potential is an interesting function to calculate in lattice gauge theory. Although genuine nonrelativistic three-quark baryons (e.g. bbb) are experimentally remote, the potential which binds them is of theoretical interest in

that it reflects some basic structural properties of $SU(3)$ gauge fields. One may inquire, for example, if the QQQ potential is well-described by a sum of two-body potentials or if there is a real three-body term. Moreover, even for light-quark mesons and baryons, the nonrelativistic quark model has met with considerable phenomenological success[4]. Thus, the pattern of levels implied by the potential model may remain approxi-

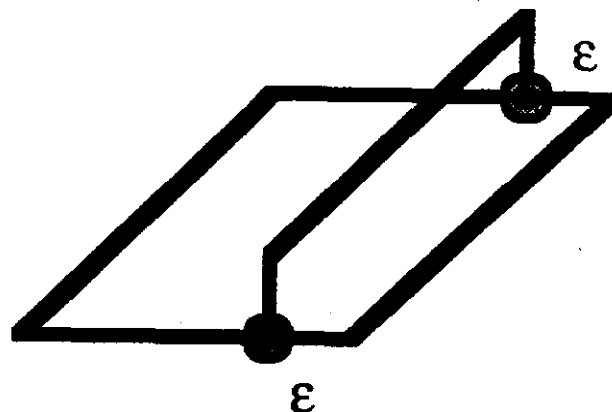


FIGURE 1

Wilson loop for the three-quark potential. The ϵ 's indicate that the color indices of the three lines are tied together with an ϵ_{abc} .

1. Fermilab is operated by Universities Research Association, Inc. under contract with the U.S. Department of Energy.

2. Supported in part by DOE grant number DOE-AC02-76ERO2220.

mately valid even for the case of ordinary light baryon resonances. The wave functions obtained from such potential model calculations may also provide interesting qualitative information on the structure of baryons. Note that it would be very difficult to directly measure excited baryon resonance masses on the lattice by the usual propagator technique, since the long-distance falloff of the three-quark propagator determines only the lightest mass state in a given channel. By instead extracting the potential from a lattice calculation and then solving the three-body Schrödinger equation, one may calculate excited energy levels precisely, albeit in the nonrelativistic approximation. (At the end of this talk, I will describe a numerical method which we have developed for determining the eigenvalues and eigenfunctions of the three-body Schrödinger operator.)

We have recently calculated the QQQ potential numerically as part of a program to study heavy quarks on the lattice [5]. The results I present here were obtained from a set of 550 $SU(3)$ gauge configurations on an $8^3 \times 16 \times 24$ lattice at $\beta = 5.7$ (lattice spacing ≈ 0.2 fm). The configurations were generated in the quenched approximation and represent a total of 60,000 Cabibbo-Marinari[6] heat bath sweeps (analyzed configurations are separated by 100 sweeps). In the calculation we introduced a variable anisotropy in the long spatial (16-) direction[7] and carried out Monte Carlo runs at five values of anisotropy, $\xi = 0.7, 0.8, 0.9, 1.0,$ and 1.1 . The introduction of anisotropy allows a more fine-grained look at the potential. (None of our results would have been substantially altered if we had analyzed only the isotropic $\xi = 1$ case.)

First, let us consider the form of $\mathcal{V}(\vec{r}_1, \vec{r}_2, \vec{r}_3)$ in the limit where two of the quarks are on the same site, e.g. $\vec{r}_1 = \vec{r}_2$. It is easy to show directly from the definition of the three-legged Wilson loop that in this limit the three-body potential \mathcal{V} reduces to the $Q\bar{Q}$ meson potential. Our results for this case are shown in Fig. 2. Fitting this two-body potential to a form $V(r) = Ar^\epsilon$ we find $A = .508$ and $\epsilon = .671$. This is more linear than the phenomenological potential extracted from the ψ and Υ spectra (for which $\epsilon \approx 0.1$). There are, of course, much more extensive calculations of the meson potential in the

literature.[1,2] Agreement with phenomenology is considerably improved by going to larger β values and by including closed fermion loop effects. The errors shown in Fig. 2 are calculated by the jackknife method[8] and are purely statistical. The Wilson loops were fit to an exponential for $t \geq 2$. This introduces some systematic error in the results of Fig. 2 at the largest separations due to non-exponential behavior. (For smaller separations ($r \leq 4$), this error is found to be small by varying the t_{\min} of the exponential fit.) A similar systematic error will also be present in the three-body data.

The full three-body potential is a function of three variables. We choose as our variables the separation $q_1 - q_2$ of the first two quarks and the transverse and longitudinal positions of the third quark relative to that axis. For purposes of visualization, Fig. 3 shows a parametrized fit to the data for a fixed value of $q_1 - q_2$. Some of the actual data points are shown in Figs. 4, 5, and 6. The horizontal-axis in these plots gives the longitudinal distance of the third quark from the midpoint of the

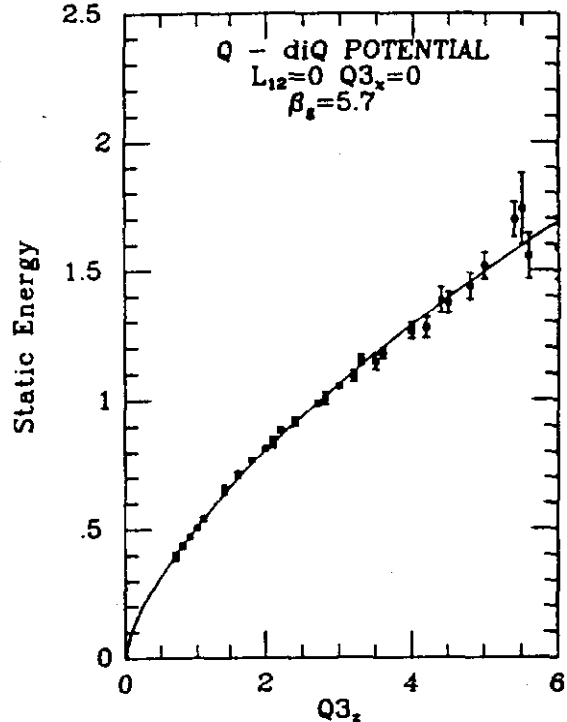


FIGURE 2

The quark-diquark potential.

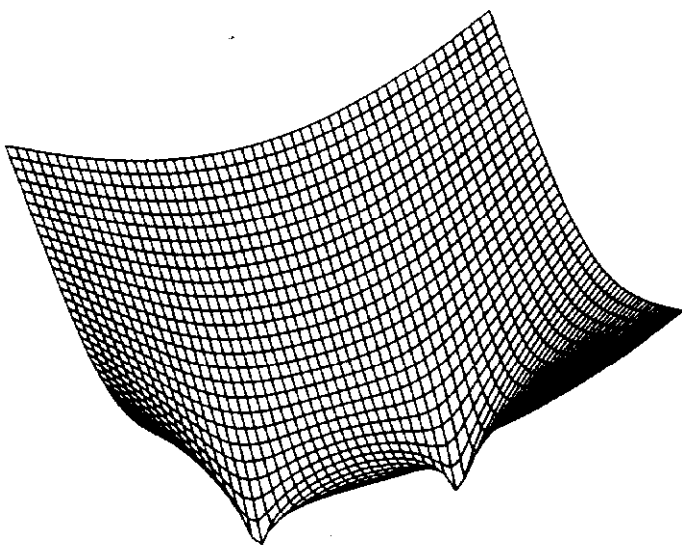


FIGURE 3

Three-quark potential V for fixed separation of quarks 1 and 2. The two horizontal axes of the 3D plot represent the location of quark 3 in a plane containing quarks 1 and 2.

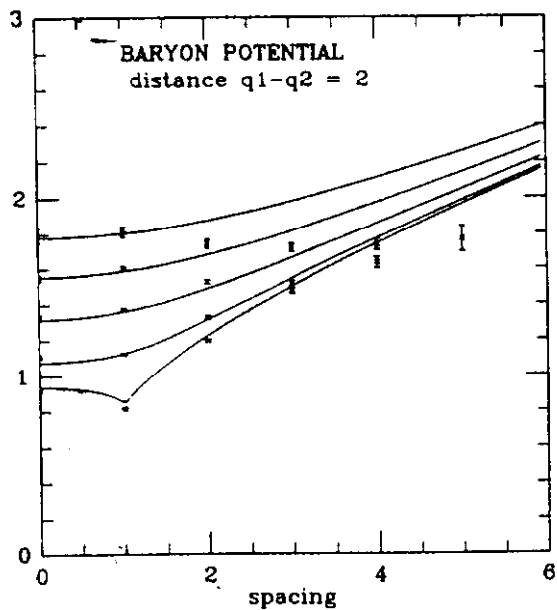


FIGURE 5

Same as Fig. 4 with $q1 - q2 = 2$.

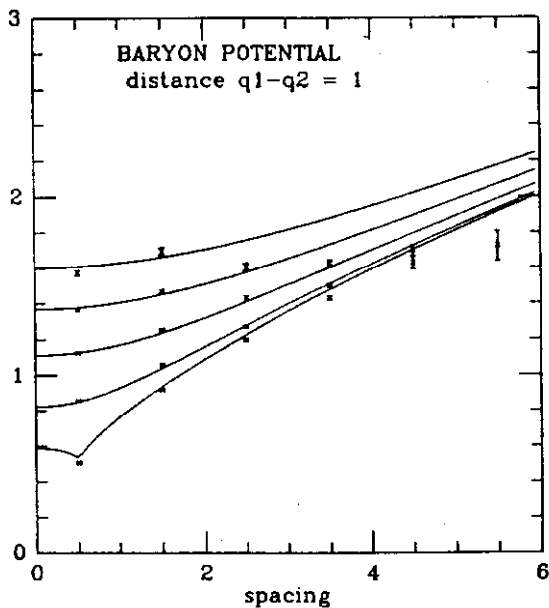


FIGURE 4

Three-quark potential for quark separation $q1 - q2 = 1$.

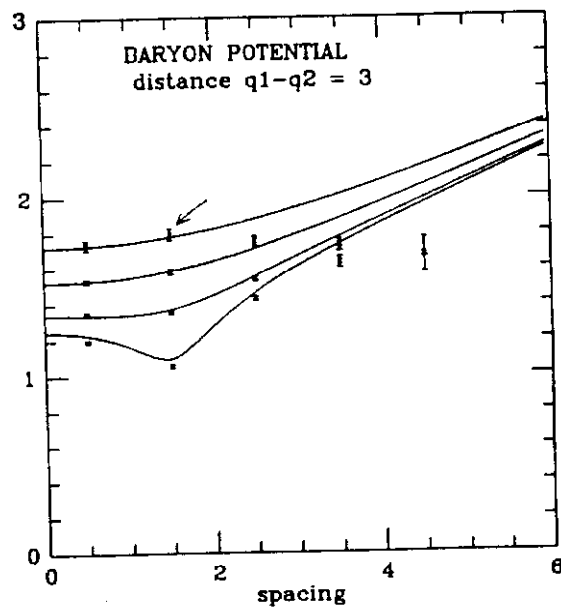


FIGURE 6

Same as Fig. 4 with $q1 - q2 = 3$.

first two. On each graph are plotted several sets of data points for different transverse separation. (To resolve possible confusion of points, note that, for example, the data sets in Fig. 4 contain 2, 3, 4, 5, and 6 points, respectively, for transverse separations of 4, 3, 2, 1, and 0.) The solid lines in Figs. 4-6 represent a comparison of the three-body data with a sum of two-body meson potentials,

$$\mathcal{V} = \frac{1}{2}[V(r_{12}) + V(r_{13}) + V(r_{23})] \quad (.1)$$

where $r_{ij} \equiv |\vec{r}_i - \vec{r}_j|$. Note that there are no free parameters in this fit, once the two-body meson potential is determined. Remarkably, this simple sum of two-body meson potentials provides an excellent description of the three-body potential over the entire range of our data. (The data points at the largest separations we measured, e.g. the points at spacing $3\frac{1}{2}$ and $4\frac{1}{2}$ in Fig. 6, do appear to deviate somewhat from the two-body fit, but as mentioned before, this is the region where we might expect some systematic error from our procedure for extracting exponential falloffs.)

The significance of the fact that (1) describes our data so well may be estimated by comparing with the predictions of the weak and strong coupling approximations. The short distance perturbative three-body potential reduces to a sum of two-body terms up to fourth order in the coupling constant,[9] and therefore, no three-body term is expected in the short distance part of the potential. On the other hand, a strong-coupling flux-tube picture, which predicts a linearly rising $Q\bar{Q}$ meson potential at large distances, gives a QQQ potential which does not decompose into a sum of two-body terms. In this model, the three-body potential is given by choosing the point where the flux tubes come together such that the sum of the distances S to the three quarks is minimized. The potential is then given by $V = \lambda S$, where λ is the slope of the linear meson potential. The deviation of this potential from a sum of two-body terms is numerically rather small,[10] but would be easily observable in our data. If C is the length of the perimeter of a triangle connecting the three quarks, then S is bounded by $\frac{1}{2}C \leq S \leq \frac{1}{\sqrt{3}}C$. Since the sum of meson potentials (1) is just $\frac{1}{2}\lambda C$, we see that the de-

viation of the strong-coupling QQQ potential from (1) is everywhere $\lesssim 15\%$ (and always positive). To take a specific case, consider the data point denoted by an arrow in Fig. 6, which corresponds to an isosceles right triangle with sides 3, 3, and $3\sqrt{2}$ in lattice units. (Note that $3a \approx 0.6$ fm.) Here, the flux-tube model would predict a positive deviation of 13% from the two-body fit, which is clearly ruled out by the data. We conclude that at the quark separations we are exploring, the flux-tube picture is not relevant.

The spectrum of energy levels of a nonrelativistic QQQ baryon is determined from the potential $\mathcal{V}(\vec{r}_1, \vec{r}_2, \vec{r}_3)$ by solving the three-body Schrödinger eigenvalue problem,

$$\left(-\sum_{i=1}^3 \nabla_i^2 + \mathcal{V}\right)\Psi \equiv H\Psi = E\Psi \quad (.2)$$

We have devised a numerical procedure for computing these eigenvalues and eigenfunctions by a conjugate gradient technique. The method may be of more general interest for treating linear eigenvalue problems, and I will briefly describe it here. First we perform an angular momentum reduction of the three-body Schrödinger operator.[11] The reduced operator is then put on a three-dimensional lattice by replacing derivatives with finite differences. (The three dimensions of the lattice represent two radial variables and one polar angle variable.) We use a conjugate gradient matrix inversion algorithm to compute the resolvent $(E - H)^{-1}$ acting on a source vector $|b\rangle$ with varying E . If the source vector has a non-zero overlap with an eigenstate of H of energy E_n , then the magnitude of the output vector $(E - H)^{-1}|b\rangle$ diverges as E approaches E_n . As one approaches E_n the output vector gives the three-body wave function for that state. In practice we have found that one can approach very close to the eigenvalues and locate their positions quite precisely. For example, Fig. 7 shows the magnitude of the output vector for a three-body harmonic oscillator potential on a 4^3 lattice. Larger lattices yield similar curves. Sample calculations on larger lattices for two-body systems and for the solvable three-body harmonic oscillator potential suggest that this technique can be used to accurately determine the spectrum of an arbitrary three-

body potential. A more detailed discussion of the spectroscopy of the lattice QQQ potential will be presented elsewhere[12]

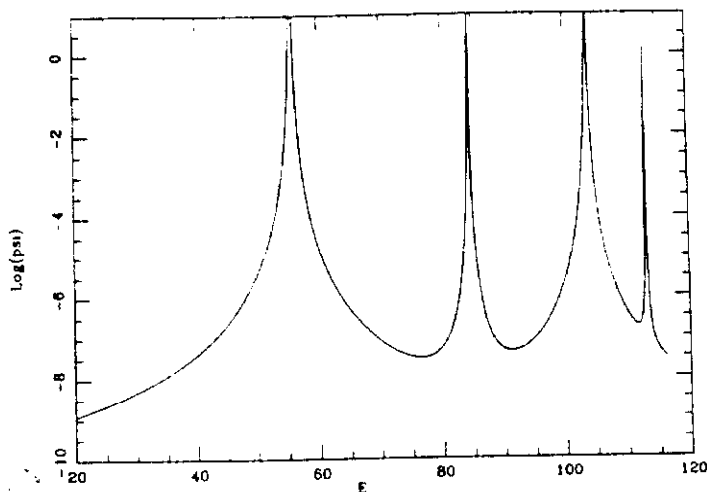


FIGURE 7

Magnitude of conjugate gradient output vector $(E - H)^{-1}|b\rangle$ for the three-body harmonic oscillator Hamiltonian on a 4^3 lattice.

References

1. J. Stack, Phys. Rev. D27, 412 (1983); S. Otto and J. Stack, Phys. Rev. Letts. 52, 2328 (1984); D. Barkai, K. J. M. Moriarty, and C. Rebbi, Phys. Rev. D30, 1293 (1984); S. Itoh, Y. Iwasaki, and T. Yoshie, Phys. Rev. D33, 1806 (1986); H. Q. Ding, Columbia preprint CU-TP-375 (1987).
2. P. de Forcrand, J. Stat. Phys. 43, 1077 (1986); P. de Forcrand, V. Linde, and I. O. Stamatescu, Freie Univ. Berlin preprint, Print-87-0595 (1987); M. Campostrini, K. Moriarty, J. Potvin, and C. Rebbi, Phys. Lett. 193B, 78 (1987).
3. Some numerical calculations have been done for this case. See J. Flower, Caltech Preprints, CALT-68-1369 (1986); CALT-68-1377 (1987); CALT-68-1378 (1987); R. Sommer, J. Wosiek, Phys. Lett. 149B, 497 (1984); Nuc. Phys. B267, 531 (1986); M. Wiltgen, Phys. Lett. 131B, 153 (1983)

4. For a review and references, see D. Gromes, Proceedings of the Yukon Advanced Study Institute, editors N. Isgur, G. Karl, and P. J. O'Donnel, World Scientific (Singapore, 1985).
5. See E. Eichten's talk in these proceedings.
6. N. Cabbibo and E. Marinari, Phys. Lett. 119B, 387 (1982).
7. J. C. Sexton and H. B. Thacker, Phys. Rev. Lett. 57, (1986) 2131
8. S. Gottlieb, P. B. MacKenzie, H. B. Thacker, and D. Weingarten, Nucl. Phys. 263, (1986) 704
9. F. L. Feinberg, Phys. Rev. D17, 2659 (1978)
10. D. Gromes and I. O. Stamatescu, Zeit. Phys. C3, 43 (1979).
11. P. M. Morse and H. Feshbach, Methods of Theoretical Physics, McGraw Hill, (New York, 1953).
12. E. Eichten, J. C. Sexton, and H. B. Thacker, FERMLAB-Pub-87/198-T